



Recent experimental explorations of non-classical nucleation

Journal:	<i>CrystEngComm</i>
Manuscript ID	CE-HIG-03-2020-000480.R1
Article Type:	Highlight
Date Submitted by the Author:	30-Apr-2020
Complete List of Authors:	Jin, Biao; Zhejiang University, Department of chemistry Liu, Zhaoming; Zhejiang University, Department of Chemistry Tang, Ruikang; Zhejiang University, Department of Chemistry

SCHOLARONE™
Manuscripts

ARTICLE

Recent experimental explorations of non-classical nucleation

Biao Jin,^{a, b} Zhaoming Liu,^b Ruikang Tang*,^b

Received 00th January 20xx,
Accepted 00th January 20xx

DOI: 10.1039/x0xx00000x

Nucleation, the early stage of crystallization, is a key step to produce functional materials, but nucleation processes have yet to be understood in detail. Recent advanced characterization techniques, especially atomic force microscopy, liquid-phase transmission electron microscopy (TEM) and cryo-TEM, enable scientists to observe previously inaccessible nucleation details at the nanoscale. In this review, we summarize newly suggested non-classical nucleation models with respect to mechanistic understanding from the experimental views, which highlight multi-steps nucleation mechanism. Different mediated phases such as clusters at pre-nucleation stage, liquid-like precursors, amorphous phase and even oligomers have been revealed, which play vital roles in nucleation and structure control. Moreover, these mediated phases practically contribute in general to the structural variances of materials for nanoscience and nanotechnology. Overall, these studies ultimately enable us to control nucleation processes for materials synthesis.

1. Introduction

Nucleation is fundamental to the formation of various materials such as proteins,¹ biocrystals² and metal nanocrystals.³ It takes place at the nanoscale with quick reactions, producing a new thermodynamic phase from a mother phase.⁴ The early stage of crystallization is always referred to as nucleation, which means an increase in local density as well as local order.⁵ In general, the nucleation of crystals is one of the most important phenomena in materials synthesis because it determines the number of crystals, the size distribution, and the polymorph selection.^{2, 6} Therefore, fundamental understandings of nucleation mechanism can provide in-depth insight for nanomaterial's synthesis, and then promoting the advanced development of material sciences.⁷

Nucleation process is greatly challenging to understand, particularly for pre-nucleation periods.⁸ This is because in typical reaction processes, nucleation occurs at the molecular/nanoscale level and within several seconds.⁹⁻¹³ To better understand nucleation process, nucleation models including classical and nonclassical pathways have been proposed based on various experimental and computational methods.⁴ The most widely used of these, classical nucleation theory (CNT) gives a suitable model to describe the nucleation rate, free energy barrier and critical nucleus size.¹⁴⁻¹⁸ Notably, the key idea of classical nucleation model is that nucleation occurs through the attachment of associated ions, atoms, or molecules to form critical nuclei.^{19, 20} However, CNT does not account for some unexpected nucleation observations proceeding through metastable/stable precursor phases including amorphous phases,²¹⁻

²⁸ clusters at pre-nucleation stage²⁹⁻³⁴ and liquid-like precursor phases³⁵⁻⁴⁴ prior to appearance of crystalline structures. Such intermediates-based nucleation is always referred to as a nonclassical nucleation pathway to distinguish it from classical nucleation.² Although classical and nonclassical nucleation models have been investigated by various methods,^{40, 45-51} the exact nucleation pathway and detailed kinetics have so far been unclear. For example, does critical nucleus size exist? Can different nucleation pathways coexist? Is the clusters-mediated nucleation pathway general across different systems? What are the roles of amorphous phase in nucleation? The key reason for these ambiguities is a lack of effective strategies and techniques to explore the details of nucleation.

The recent development of advanced characterization techniques, such as in situ atomic force microscopy (AFM),^{10, 52} liquid-cell transmission electron microscopy (TEM)⁵³ and cryo-TEM,^{54, 55} enables us to investigate nucleation dynamics and intermediate stages at nanoscale. In this review, we focus on recent experimental evidence to advance the nanoscale-level understanding of nucleation mechanisms of nanocrystals in solution, which reveal that nucleation is a very complicated process, rather than a simple process as described by CNT.⁵

2. Nucleation without free energy barrier

In CNT, the negative chemical potential upon nucleation and positive surface tension give rise to a free energy barrier and a critical size.⁵⁶ CNT predicts that the nucleation of 2D islands requires a critical size by overcoming the free energy barrier, which has been experimentally demonstrated in the glucose isomerase crystals and ice nucleation process.^{57, 58} However, recent work shows that critical size and free energy barrier in CNT are not necessary for the formation of 2D arrays.¹⁰ As shown in Figure 1, *in-situ* AFM observations of the pathway and kinetics of 2D molecular arrays

^a Physical Sciences Division, Pacific Northwest National Laboratory, Richland, WA 99352, USA

^b Department of Chemistry, Zhejiang University, Hangzhou, Zhejiang 310027, China

† Footnotes relating to the title and/or authors should appear here.

Electronic Supplementary Information (ESI) available: [details of any supplementary information available should be included here]. See DOI: 10.1039/x0xx00000x

formation on MoS₂ interface show that the peptides attach to the surface and directly grow into ordered structures (Figure 1a). Additionally, the nuclei tend to grow along preferential lattice directions to form elongated island structure (Figure 1b, c). There is no evidence showing the existence of a metastable transient phase or cluster attachment process. Further, the simulation of single peptides and circular dichroism spectra find that MoSBP1 always remains in monomeric state in bulk solution. These results imply that the assembly process can be conceived as a continual nucleation process of 1D nucleus via monomer attachment. To understand the energetic controls during the assembly process, the measurements of nucleation rates at different peptide concentrations and along different growth directions find that nucleation start as soon as peptide concentration (c) exceed island solubility limit (c_e) with a nucleation rate ($J_n \propto c$) and critical island size reaches zero at c_e (Figure 1d-f). These results agree with long-standing but unproven predictions of CNT in 1D that the nucleation of 1D structures takes place without a free energy barrier. In fact, nucleation is not only controlled by a free energy barrier,⁵⁶ it is also associated with a kinetic activation barrier which is based on the molecular-level processes, such as desolvation and ions binding.⁵⁹ Because nucleation rate depends on both the free energy barrier and activation barrier. Thus, even if without free energy barrier, the activation barrier can ensure that nucleation events occur. In view of these findings, the understanding of nucleation mechanisms should also consider the kinetic activation barrier that determines the frequency of nucleation, which is different from free energy barrier that enables the system to explore all the possible structure configurations and control the probability of forming a cluster larger than the critical size.

3. Multi-step nucleation

Nonclassical nucleation pathways have attracted a great deal of interest because of their widespread practical importance in nanoscience and nanotechnology.² The nucleation of crystals is accompanied by improvements both in local density and order as well as increasing size. Consequently, we can classify different intermediates from these parameters and their formation pathway. For example, the size of cluster at pre-nucleation stage and amorphous phase is different; the density of liquid-like precursor phase and amorphous phase is distinguished despite that they are disordered structure. Here, we grouped them into several categories: cluster-, liquid-like precursor phase-, amorphous phase-, and primary-particle-mediated nucleation, which can be referred to as multi-step nucleation. Although amorphous intermediated phases have been reported in variety of systems,^{21-26, 48, 60-62} the early stages of nucleation remain less clear considering the existence of more complicated precursor structures. With recent advanced explorations of crystallization process, the nucleation of nanocrystals is extended to clusters mediated pathway.³⁴ Besides, polymer induced liquid phase (PILP)³⁹ and dense liquid phase (DLP)⁴³ appear in the pre-nucleation/nucleation periods. Due to their highly dynamic and transient or ultra-small species, it is a great challenge to

directly investigate the multi-step nucleation process occurring in solution. But in situ microscopy techniques have been proven to be reliable strategies to probe the underlying nucleation mechanism by capturing the transient and nanoscale precursors.^{12, 25, 59, 63 64 30} Experimental evidence revealed by advanced characterization techniques provides a more complete and clearer picture of nonclassical nucleation mechanism.

3.1. Cluster-mediated nucleation

The existence of thermodynamically stable solute species has been presented, e.g. multimeric clusters,⁶⁵ that can disperse in homogeneous solution without phase boundary.³⁴ The clusters at pre-nucleation stage are observed as building units to produce a new phase. These clusters are believed to be molecular precursors to the phase nucleating from solution, and finally take part in the phase separation process.^{8, 66} From these experimental observations, it is speculated that clusters-mediated nucleation may be an important pathway in multi-step nucleation.

The clusters are often termed pre-nucleation cluster (PNC) during the formation process of calcium carbonate (CaCO₃),^{34, 49, 67-70} calcium oxalate,⁷¹ calcium phosphate,^{31, 33, 72-74} iro(oxy)(hydr)oxide^{29, 75, 76} and CaSO₄.⁷⁷ The existence of CaCO₃ PNCs was firstly inferred from potentiometric titrations, analytical ultracentrifugation and cryo-TEM.^{34, 78} The possible structural forms of CaCO₃ PNCs are proposed to be chains-, rings- and branch-like structures by simulations.⁷⁹ And the concentration of ions can affect the structure of PNCs via changing the balance of equilibria and the frequency of collision. For example, these PNCs with chain-like structure can be observed at different concentrations of ions, but the branch structure is very rarely to be found at the lower concentration.⁷⁹ Notably, the exact correlation between concentration and atomic configuration of PNCs fails to be built, which require more computational and experimental explorations. Also, some isolated nanometre-sized calcium phosphate PNCs are observed and aggregate to a loosely networked structure (Figure 2a) prior to apatite formation.³³ But it is extremely difficult to directly visualize the structure, formation pathways of these clusters at pre-nucleation stage, which greatly relies to computational methods.^{74, 80, 81} Using comprehensive free energy calculations, it is suggested that the consecutive coordination of phosphate to calcium ions results in the formation of PNCs, which is mainly consisted of the most stable ion association complex-Ca(HPO₄)₃⁴⁻.⁷⁴ And highly charged species play a key role in stabilizing PNCs and their aggregates. In addition, PNCs are further probed in other systems. For instance, PNCs are also existed in iro(oxy)(hydr)oxide system^{29, 75, 76, 82} where iron (III) oxide nucleates through the formation and aggregation of iron (III) (oxyhydr)oxide PNCs (Figure 2b, c).⁷⁶ Moreover, cryo-TEM study on the post-nucleation stage of hematite implies the existence of PNCs (Figure 2d).²⁹ These studies signify the importance of PNCs in crystal nucleation.

However, the PNC model has received some challenges due to the difficulties of directly detecting the existence of PNCs in solution. Therefore, it is still hard to show if PNC is a reliable and accurate

model to describe nucleation process of these systems. For example, study shows that ion pairs and polynuclear complex are key species in calcite system,⁸³ which does not support the PNC model. In addition, it is found that the initial stages of CaCO₃ nucleation in supersaturated solution are dominated by ions and ion pairs with no involvement of PNCs, as expected from CNT.⁸⁴ With these different evidences, it is very necessary to re-evaluate the PNC model in different systems using advanced experimental and computational methods, at least in CaCO₃ system.

On the other hand, magic-size clusters (MSCs) are also reported, which occur as key intermediates at the pre-nucleation stage of colloidal semiconductors.⁸⁵ MSCs is a kind of transition structures connecting molecules and nuclei.⁵¹ The stepwise growth from MSCs directly to quantum dots proceeds through either an aggregation process⁸⁶ or a second nucleation event.⁸⁷ Interestingly, the type of MSCs from one pre-nucleation stage is different. For example, in the synthesis of CdTe quantum dots, two different MSCs as intermediates appear prior to their nucleation, which supports multi-step nucleation model.⁸⁶ And certain types of MSCs can be converted into other MSCs.⁸⁸ These cases suggest that MSCs mediated nucleation process is much more complicated than the picture in CNT.

Overall, PNCs are stable species in solution at any concentration, including unsaturated solution. They are different from classical pre-critical clusters which are unstable species that exist in any solution at any concentration. However, MSCs are metastable nucleated species where they sit lies at a special size and atomic configuration. These various clusters imply the complicated energetics, enriching the nucleation pathway.

3.2. Liquid-like precursor phase in nucleation

A liquid-like precursor phase is now recognized as an important intermediate in the nucleation process of nanocrystals, especially for biominerals^{37, 39, 89-91} and proteins.^{41, 42, 92, 93} Such precursor phase can be understood from its disordered structure and concentrated solute aggregates with liquid-like characteristic. A typical case is so-called polymer-induced liquid precursor (PILP), which contributes to the formation of crystals with non-equilibrium morphologies.^{38, 94-97} For example, in the presence of charged polymers, PILP of CaCO₃ formed, then coalesced to form thin films on substrate, and finally transformed into calcite or vaterite.^{38, 95} A PILP process has been found in the barium carbonate,⁸⁹ calcium phosphate⁹⁸ and amino acid systems.⁹⁴ Taking CaCO₃ as a model system, PILP is investigated from its liquidity, deformability, and gel-like elasticity by the quantitative self-diffusion efficient measurements, SEM, cryo-TEM and in situ AFM.^{35-37, 39, 99} With these characteristics, Mg ions are used to tune the wettability of PILP of CaCO₃, and thus controlling its mineralization site in hybrid materials.¹⁰⁰ While these studies described the special properties and key roles of PILP, its microscopic structure remains unclear. Sommerdijk. et al. used high-resolution cryo-TEM to reveal the microstructure of PILP of CaCO₃; the PILP phase consists of 30-50 nm ACC nanoparticles including ~2 nm nanoparticulate texture (Figure 3a).¹⁰¹ This suggests that PILP is a

polymer-driven assembly of amorphous clusters in substance, and the liquid-like behaviour of PILP at macroscopic/mesoscopic scale derives from the small size and surface properties of the dynamical assemblies of ~2 nm-sized ACC clusters stabilized by charged polymers. Notably, no obvious evidence shows that liquid-liquid phase separation is responsible for the formation of the PILP. The role of polymers in PILP process is to enhance the stabilization kinetics of PILP; this role highlights the effects of polymers as a method for preparing minerals with complicated structures, such as the remineralization of osteoporotic bones.⁹⁸ As shown in Figure 3b, a free-flowing calcium phosphate PILP is stabilized on a large scale and at a high Ca²⁺/PO₄³⁻ concentration. The microstructure of such calcium phosphate PILP includes a high density of uniform-sized ACP nanoclusters (Figure 3c). This PILP material has excellent bone inductivity, and thus promotes intrafibrillar mineralization of collagen fibrils.⁹⁸ Additionally, a process similar to PILP has also been observed in purely inorganic systems, e.g., a condensed phase of liquid-like droplets of CaCO₃ can form at a critical concentration without polymers.⁹⁹ This evidence confirms that the PILP process represents the assembly behaviour of nanoclusters driven by polymers and the liquid-like precursor phase consists of polymer-stabilized rather than polymer-induced species.^{98, 101}

Based on these understandings, a liquid-like precursor phase with a more general concept, that is dense liquid phase (DLP), is developed.^{42-44, 93, 102} Extensive studies show that the nucleation of protein crystals under certain conditions proceeds in two distinct steps: the formation of a DLP and followed by the nucleation of ordered protein structure within the liquid phase.^{43, 103} The DLP of protein is liquid dense protein clusters, which are liquid-like and stable with respect to the mother phase and metastable relative to the final crystalline phase.⁹³ The DLP of CaCO₃ is also formed in supersaturated solutions through the association of ions and ion pairs without significant participation of larger ion clusters, which then act as precursor of vaterite.¹⁰⁴ During vaterite growth process, it is achieved through a net transfer of ions from surrounding solution, stressing a classical concepts of crystal nucleation and growth, which is applicable to describe multistep nucleation mechanism here. The structure, dynamics, and energetics of hydrated CaCO₃ clusters is explored using molecular dynamics simulations, which found that dense liquid clusters phase formed through liquid-liquid separation in supersaturated solution.¹⁰⁵ During this model, the DLP of CaCO₃ is metastable relative to all solid phases because a liquid-liquid coexistence line exists between the DLP and the ion-poor solution phase. And DLP through liquid-liquid separation includes small cluster population which is stable in a statistical sense. Subsequently, the coalescence and solidification of nanoscale droplets result in the formation of ACC. This finding is consistent with ACC nanoparticles being produced from the dehydration and solidification process of liquid-like precursor. It is also revealed that nucleation occurs within the dense and disordered urea clusters.⁷⁰ But so far, the data about exact location of formation of the solid phase in DLP is limited, which requires more studies.

Moreover, the formation of DLP is based on a liquid-liquid phase separation mechanism that results in solute-rich and solute-poor

liquid phases followed by the formation of nuclei in a solute-rich liquid phase.¹⁰² Using in situ high resolution liquid-cell TEM, Mirsaidov et al. revealed the multiple nucleation process of Au nanocrystals in aqueous solution via three stages (Figure 4): liquid-liquid separation into solute-rich and solute-poor liquid phases, nucleation of amorphous nanoclusters within the metal-rich liquid phase, and crystallization of these amorphous clusters.¹⁰⁶ This multistep nucleation pathway via DLP helps to develop broadly applicable nucleation models. Further, it is suggested that the formation of liquid droplets is entropy driven while the subsequent nucleation is mediated by enthalpic interactions.¹⁰² By building a diffusion-limited nucleation model of macromolecules in solution for liquid-liquid separation, it is suggested that an excess of matter must come together via some fluctuations to form a dense droplet, which is unstable before growing to a critical droplet.¹⁰⁷ Despite that the nucleation begins by the formation of liquid droplets, the solid phase does not form via a nucleation event within a metastable, growing droplet.¹⁰⁷

3.3. Amorphous phase in nucleation

Both clusters- and liquid-like precursor phase- mediated nucleation pathways involve an amorphous phase before crystal formation. In a typical 2D colloid crystallization system, an amorphous dense phase is first nucleated because of its lower nucleation energy barrier compared with crystals which results from their lower interfacial energy, and the second step is the nucleation of a crystalline phase within a metastable amorphous phase.^{26, 27} Such nonclassical features of nucleation have also been found in various nanocrystal systems.^{12, 23, 48, 61, 62, 108, 109} For example, an amorphous precursor phase appears before metal-organic frameworks (MOF),¹¹⁰ calcite,⁵² and hydroxyapatite⁶² formation.

In the classical nucleation model, nucleation is believed to be mainly controlled by the free energy barrier so that the formation of amorphous phases would be more likely than the crystalline phase at exactly same supersaturation due to their lower surface energy.⁵⁶ However, TEM studies of the early stage of crystallization show that nucleation is initiated by the formation of amorphous phases that are subsequently nucleated into the crystalline phase.^{24, 111-113} For example, cryo-TEM investigation shows that amorphous calcium silicate spheroids in the calcium silicate hydrate nucleation process form and then transform to crystalline tobermorite-type C-S-H via sodium/calcium cation exchange and aggregation process.²² However, uncertainty still exists as to whether the most stable crystalline phase directly nucleates from solution or forms through an amorphous precursor phase. Luckily, the amorphous phase can be observed in which the nucleation process of both aragonite (Figure 5a) and vaterite (Figure 5b) in aqueous solution can be achieved via the phase transformation of ACC by in situ TEM.²⁵ Notably, the stability of amorphous phases is always controlled by additives.⁶² However, how additives affect the nucleation of the crystalline phase from amorphous phase remains insufficiently understood.

To investigate the roles of additives in amorphous phases mediated nucleation, some remarkable works have been presented.

For example, liquid-cell TEM investigation of the nucleation of CaCO₃ in a matrix of polystyrene sulphonate (PSS) shows that direct nucleation of vaterites occurred without PSS (Figure 5c), but amorphous ACC can form in the presence of PSS at the same supersaturation conditions (Figure 5d).⁵⁹ ACC nucleation in the presence of PSS and vaterite nucleation in its absence occur at higher and lower local supersaturation degree estimated by time resolved TEM analysis, respectively. This means that PSS increases local supersaturation, resulting in ACC nucleation only at the sites of the globules. These observations show that Ca²⁺ ions binding to form Ca-PSS globules (Figure 5e) drive CaCO₃ nucleation via forming metastable ACC. The specific ions binding with the polymer sulphonate groups ensures that the nucleation of ACC occurs within the globules considering that ions binding-based kinetic barrier can increase the local supersaturation. These analyses of nucleation events in the presence of PSS demonstrate the nucleation energy barrier not only depends on the free energy barrier, but it is also controlled by a kinetic barrier associated with atomistic processes, such as ions binding.

Additionally, in situ AFM experiments find that the nucleation of calcite in the absence of organic molecules occurs via an interface-coupled dissolution-recrystallization process of ACC, whereas in the presence of organic molecules it retains the nanogranular texture of the colloidal growth layer, presumably via direct rearrangement.⁵² Meanwhile, recent time-resolved cryo-TEM investigation also shows that the nucleation of zeolitic imidazolate framework 8 (ZIF-8) is achieved via dissolution and recrystallization of highly hydrated amorphous particles, but a direct solid-state transition process occurs with the assistance of protein, which finally results in the different morphologies of ZIF-8.¹¹⁰ But it is unknown that how additives alter products shape, which is demonstrated by recent liquid-cell TEM investigation. It is found that Mg ions can regulate the phase transformation pathway from ACC to calcite in a concentration-dependent manner (Figure 6).^{13, 114} Specifically, without Mg ions, the dissolution-recrystallization pathway is dominant (Figure 6a), whereas a direct transformation occurs in the presence of Mg ions via the nucleation of calcite within ACC and dehydration, leading to the formation of calcite via preserving the original spherical shape (Figure 6b). The altering of the pathway is attributed to the Mg ions enhancing hydrogen-bonded networks between CO₃²⁻ and water molecules that promote the ion rearrangement within ACC particles. Here, the effect of the confinement environment in the liquid-cell is less considered despite that confinement effect is significant on the stability of ACC.^{115, 116} With these understandings, it is suggested that additives play important roles in regulating the varieties of crystalline morphologies, polymorphs, and structures during amorphous phases mediated nucleation process.¹¹⁴ For example, a spinodal decomposition of the Mg-ACC precursor into Mg-rich nanophases and a Mg-depleted amorphous phase and subsequent crystallization can produce a single-crystal Mg-calcite layer.¹¹⁷ And ACC can transform into vaterites and calcite dominant products in the presence/absence of ethanol, respectively.¹⁰⁸

The predicted lower surface energies of amorphous particles hint at the generality of the amorphous precursor-mediated nucleation mechanism in various systems. The nucleation of metal nanocrystals in solution is rarely investigated at the nanoscale due to techniques limitations. Using high-resolution electron tomography and graphene liquid cell, the 3D structure of individual Pt nanocrystals at near-atomic resolution has revealed that a single nanocrystal includes multiple crystalline domains,⁶⁰ presumably from multiple coalescence events in the early stages of the nanoparticle formation process. However, it remains unknown whether the nanocrystals are produced from the initial aggregation of small clusters. The direct observation of the Ni nanocrystal formation process by graphene liquid-cell TEM reveals a different mechanism via two-steps: an amorphous phase is rapidly formed from the initial homogeneous precursor solution, and then a crystalline nucleus appears within the amorphous phase (Figure 7a, b). Following that, the nucleus grows into a large crystal with the expense of the amorphous phase.¹² Interestingly, the sequential nucleation of multiple crystalline grains in the one amorphous particle is also observed (Figure 7c). The coexistence of three different crystalline domains with sharp interfaces implies that the formation of multiple crystalline grains in amorphous-phase-mediated crystallization can be an alternative pathway to synthesize multi-grained nanocrystals.

Another important question is how these amorphous phases are involved in nucleation process. Most literatures show that the amorphous phase acts as precursor for subsequent nucleation, such as the nucleation of hydroxyapatite from ACP.^{45, 62} However, this understanding is different from observations of the nucleation of lysozyme crystals.⁶¹ Using time-resolved liquid-cell TEM, an amorphous spherical particle nucleates from supersaturated solution that as precursor transforms into an orthorhombic crystal (Figure 8a). Another amorphous particle can also form around the existing particles, develop some small facets and finally transform into crystalline particle (Figure 8b). These results indicate that solid amorphous particles are not only precursors, but also work as heterogeneous nucleation sites or templates for enhancing the nucleation event. Additionally, in situ AFM reveals ACC as grow units in the formation of calcite, which involves a layer-by-layer attachment of ACC particles.⁵² These different findings remind us to re-consider the roles of amorphous phases in nucleation process.

These advances in the mechanistic understanding of amorphous phase-mediated crystalline phase formation can direct the synthesis of functional materials because the controlled stability of amorphous phases via additives and reaction conditions enable us to effectively regulate phase transformation and aggregation processes. Notably, the amorphous phase provides the possibility to tailor nanocrystals with unpredicted morphologies that are challenging to synthesize by conventional methods. For example, amorphous phases can be used to prepare crystals with hierarchical structures.¹¹⁸⁻¹²⁰ But the types of amorphous phases can vary from certain conditions, such as ACC with different hydration amounts,¹²¹⁻¹²⁴ which complicates the subsequent nucleation process of crystalline phase. Therefore, more explorations of the amorphous phase are necessary.

3.4. Primary particles for nucleation

In addition to previous PNCs, sometimes primary particles can be regarded as a stable precursor phase for the nucleation of a new phase. For example, the formation of gypsum experienced three distinct stages by quenching reaction and high-resolution TEM: (1) the homogeneous nucleation of crystalline hemihydrate bassanite under its predicted bulk solubility; (2) the self-assembly of basanite into elongated aggregates along the preferential *c*-axis, and (3) the nucleation of dihydrate gypsum by solid-state transition.¹²⁵ In this case, the stable nanocrystalline precursor phase and their self-assembly provide an effective pathway for the formation of gypsum. Further, in situ fast time-resolved small-angle X-ray scattering reveals the nucleation of gypsum is achieved by the aggregation of sub-3 nm primary species.¹²⁶ A similar process is also demonstrated in the magnetite system, in which disordered primary particles were observed.^{6, 54} Using cryo-TEM, the nucleation and growth of magnetite was showing to be through the rapid aggregation of nanometric primary particles. Note that in contrast to the cases in calcium carbonate/phosphate where amorphous bulk phase was formed via PNCs attachment.⁵⁴ there is no evidence of an amorphous intermediate bulk precursor phase in the formation of magnetite nanocrystals. Further, the thermodynamics and the kinetics of the crystallization process of magnetite can be described within the framework of colloidal assembly.⁶ In the early stage, crystalline iron(oxy)-hydroxide particles are formed (Figure 9a), and then aggregate to form clusters (Figure 9b). At a later stage, when an intermediate phase becomes favourable above a critical size, the conversion to magnetite occurs (Figure 9c). Based on these observations, a kinetic model based on colloidal assembly is built to quantify the aggregation of primary particles. From this model, the number and average size of crystal at a given initial Fe concentration is readily predicted. This work not only stresses the intersection of crystallization theory and colloidal theory to give a deep understanding of nonclassical nucleation mechanisms, but also provides a new idea on the controlled preparation of nanocrystals with predefined sizes. However, for the primary particle-mediated nucleation pathway, the interaction potential between primary particles plays a key role by considering the interplay of thermodynamic and kinetic factors.¹²⁷ More investigations of primary particle-mediated nucleation mechanism need to be done in the future.

3.5. Cluster-mediated particle relaxation in nucleation

As described above, the diversity and complexity of non-classical nucleation and crystallization pathways of nanocrystals has been investigated in situ at the nanoscale. Using liquid-cell TEM, the microscopic nucleation process of palladium nanocrystals involves an intermediate state of condensed atomic clusters, which is named a "cluster-cloud" structure (Figure 10). Initially, some ultra-small clusters are produced from homogeneous solutions (pre-nucleation periods) (Figure 10a). These clusters are highly hydrated and

stabilized by water molecules, which can aggregate to form a condensed cluster-cloud structure (Figure 10b). Due to the instability of the cluster-cloud, nucleation is initiated by its quick collapse, followed by the formation of a nanoparticle (nucleation periods) (Figure 10c-d). However, this particle is a poorly crystallized structure. The subsequent maturation occurs via a multiple out-and-in rearrangement process, producing more ordered crystalline structures (post-nucleation periods) (Figure 10e). Combining experimental observation and atomistic simulations, it is believed that the hydrated clusters and cluster-cloud-mediated nanocrystallization demonstrates an order-disorder phase separation and reconstruction during the nanocrystal formation process. Such hydrated clusters and cluster-cloud based nucleation process suggest a distinguished multi-step nucleation mechanism. The key difference is that the maturation contributes greatly to the order improvement of nanocrystal. This expanded multi-step nucleation mechanism not only enriches nonclassical nucleation models, but also grants new strategy for nanomaterials preparation.

4. Inorganic polymerizations and crosslinking

Besides traditional multi-step nucleation models highlighted above, monomer and oligomer molecules are also involved in nucleation processes as important precursors in polymers. Typically, "oligomer" refers to a molecular complex that has less than ten repeated monomer units.^{128, 129} These oligomer structures can produce a crystalline material with specific structure, e.g., nematic liquid crystal drops.¹³⁰ This concept can be extended to inorganic systems. For example, with silica as one of the minerals, the covalent Si-O-Si bonds with SiO₄ tetrahedra as the basic structural motif are responsible for stability of the silica oligomers that form from a series of coupled condensation/hydrolysis and protonation/deprotonation reactions. With these silica oligomers, monolithic silica and silica-based glasses,¹³¹ even more complicated silica structures have been successfully prepared.¹³²⁻¹³⁷ It is likely that the polymerization via monomer and oligomer precursors plays an important role in material formation. However, the existence of ionic oligomers as basic building units for materials formation is minimally reported in literature.

Using CaCO₃ as a model, an ionic polymer-like structure of CaCO₃ has been successfully synthesized by using ethanol as the solvent.¹³⁸ The capping of triethylamine (TEA) is used to stabilize the precursors, which is defined as (CaCO₃)_n ionic oligomers (Figure 11a), as described in silica system. The basic units' number within ionic oligomers is adjustable between 3-11 via altering the molar ratio of calcium ions to TEA (Figure 11b). By using synchrotron small-angle X-ray scattering to analyse the monodispersed oligomers solution, it is revealed that the oligomers are rod-like structure with a length of approximately 1.2 nm (Figure 11c). These oligomers can follow a stepwise chain-like or branch-like once removing the TEA (Figure 11d), and this process is very similar to polymerization in polymer chemistry. If the density of oligomers density is increased, the crosslinking of ionic oligomers leads to the rapid construction of a pure monolithic ACC (Figure 11e), and even produces crystals with a

continuous and oriented internal structure (Figure 11f). This polymerization and crosslinking from oligomers to chains, networks and final bulk materials can be regarded as a phase-separation mediated nucleation process (Figure 11g), which is obviously different from any previous nucleation models. Moreover, the fluid-like property of oligomer precursors enables it to be moulded into specific shapes from nanometre to centimetre scale. Using a similar method, the ultra-small calcium phosphate oligomers are obtained and successfully used to repair the damaged tooth enamel.^{138, 139} From these results, crosslinking ionic oligomers as conformable precursors shows their great potentials to prepare inorganic materials, which demonstrate the special advantage of combining classic inorganic and polymer chemistry in nucleation. Generally, this phenomenon stresses that the polymerization and crosslinking of oligomers promotes the phase-separation, which dominates the nucleation of a new phase.

5. Conclusions and perspectives

In conclusion, there are vast experimental evidence showing the coexistence of multiple nucleation pathways of nanocrystals in solution (Figure 12). Although most of these models were revealed in earlier works as a result of the speculations of experimental phenomena, we highlight the vital role of time-resolved techniques in coupling these nucleation models at the nanoscale.^{6, 10, 12} In pre-nucleation periods, dynamic clusters are formed by partial hydration water loss of hydration ions, which are thermodynamically stable relative to initial ion states.⁶⁹ The decreasing of clusters dynamics due to further dehydration may result in formation of a liquid-like precursor phase. Then, condensation of the liquid-like precursor phase accompanied with dehydration and aggregation produces an amorphous phase which finally transforms into the crystalline phase. The critical role of water and other solvents in these non-classical views on nucleation^{67, 140} is often neglected. Additionally, the findings of primary particle-mediated nucleation,⁶ cluster-mediated particle relaxation,¹⁴¹ and inorganic polymerization and crosslinking of oligomers¹³⁸ further advance our detailed understanding of the nucleation mechanisms. However, further studies of nucleation models are required to address the following questions and challenges:

- (1) In non-classical nucleation models, what are the effects of pH, precursor concentration and additives on nucleation pathways? How can the specific nucleation pathway be controlled? How can we predict which nucleation pathway is dominant when given a certain condition?
- (2) What are the roles of the amorphous phase in crystal formation? Is the formation of amorphous phases from liquid-like precursors a result of nucleation or simply dehydration or direct rearrangement? What is the relationship between clusters at pre-nucleation stage, liquid-like precursors, and the amorphous phase?
- (3) Do morphologies and structures of nanocrystals depend on the form of precursors? If so, how do these precursors control the polymorphism?

- (4) Present nucleation models are mainly based on homogeneous nucleation studies. If heterogeneous nucleation and chemical reactions are considered, how could suitable models describe the complicated nucleation kinetics? Further, what are the roles of interfacial structures on the nucleation sites?
- (5) Assuming multiple metastable states as intermediates exist, how can their nucleation energy barrier and rate be evaluated from complex free energy? At the early stage of nucleation, how do these multiple metastable intermediates transform each other?
- (6) How do ionic oligomers form and how do they evolve into a crystal?

Obviously, these challenges require advanced characterization techniques with high temporal and spatial resolution. Considering that every technique has its advantages and limitations, the coupling of different complementary techniques, as exemplified by the combination of in situ ATR-IR and liquid cell TEM,¹³ will be an excellent strategy. By combining these advanced techniques, it is possible to obtain either morphological or structural, and either collective or localized information,¹⁴² which will assist us to reconstruct the entire scheme of nucleation mechanisms. In conjunction, computational methods can reveal nucleation details at the atomic level, which is inaccessible to most existing experimental techniques.⁷⁴ However, most molecular simulations and calculations cannot yet tractably address real experimental conditions, and instead address simplified conditions, e.g., with much shorter time scales than those of real nucleation process.¹⁴³

Further mechanistic understanding of nucleation based on advanced techniques will greatly advance our ability to synthesize materials with superior physical and chemical properties. Although the established nucleation models can be used to explain the formation of complex crystalline materials, it is still challenging to direct the synthesis of nanomaterials for scientific and industrial applications. The crucial importance of the controlled synthesis of stable precursors to a broad range of high-performance materials applications validates the significance of nucleation model studies.

Competing Interests

The authors have declared no competing interest.

Acknowledgements

We thank James J DeYoreo for the useful discussions and suggestions. This work was supported by the National Natural Science Foundation of China (Grant No. 21805241) and Pacific Northwest National Laboratory (PNNL), operated for the U.S. Department of Energy by Battelle under Contract DE-AC05-76RL01830.

Notes and references

- 1 M. Sleutel and A. E. Van Driessche, *Nanoscale*, 2018, **10**, 12256-12267.
- 2 M. Jehannin, A. Rao and H. Cölfen, *J. Am. Chem. Soc.*, 2019, **141**, 10120-10136.
- 3 N. T. Thanh, N. Maclean and S. Mahiddine, *Chem. Rev.*, 2014, **114**, 7610-7630.
- 4 S. Karthika, T. K. Radhakrishnan and P. Kalaichelvi, *Cryst. Growth & Design*, 2016, **16**, 6663-6681.
- 5 J. Lee, J. Yang, S. G. Kwon and T. Hyeon, *Nat. Rev. Mater.*, 2016, **1**, 1-16.
- 6 G. Mirabello, A. Ianiro, P. H. H. Bomans, T. Yoda, A. Arakaki, H. Friedrich, G. de With and N. Sommerdijk, *Nat. Mater.*, 2019, 1-6.
- 7 S. Yao, B. Jin, Z. Liu, C. Shao, R. Zhao, X. Wang and R. Tang, *Adv. Mater.*, 2017, **29**, 1605903.
- 8 D. Gebauer, M. Kellermeier, J. D. Gale, L. Bergstrom and H. Cölfen, *Chem. Soc. Rev.*, 2014, **43**, 2348-2371.
- 9 M. Liu, K. Wang, L. Wang, S. Han, H. Fan, N. Rowell, J. A. Ripmeester, R. Renoud, F. Bian, J. Zeng and K. Yu, *Nat. Commun.*, 2017, **8**, 15467.
- 10 J. Chen, E. Zhu, J. Liu, S. Zhang, Z. Lin, X. Duan, H. Heinz, Y. Huang and J. J. De Yoreo, *Science*, 2018, **362**, 1135-1139.
- 11 A. E. S. Van Driessche, N. Van Gerven, P. H. H. Bomans, R. M. Joosten, H. Friedrich, D. Gil-Carton, N. A. J. M. Sommerdijk and M. Sleutel, *Nature*, 2018, **556**, 89-94.
- 12 J. Yang, J. Koo, S. Kim, S. Jeon, B. K. Choi, S. Kwon, J. Kim, B. H. Kim, W. C. Lee, W. B. Lee, H. Lee, T. Hyeon, P. Ercius and J. Park, *J. Am. Chem. Soc.*, 2019, **141**, 763-768.
- 13 Z. Liu, Z. Zhang, Z. Wang, B. Jin, D. Li, J. Tao, R. Tang and J. J. De Yoreo, *Proc. Natl. Acad. Sci. U S A*, 2020, **117**, 3397-3404.
- 14 R. Becker and W. Döring, *J. Ann. Phys.*, 1935, **24**, 752.
- 15 M. Volmer and A. Weber, *Z. Phys. Chem.* 1926, **119**, 277-301.
- 16 J. W. J. Gibbs, *Amer. J. Sci.* 1878, **96**, 441-458.
- 17 D. Kashchiev, *J. Chem. Phys.*, 2006, **125**, 014502.
- 18 C. N. Nanev, F. V. Hodzhaoglu and I. L. Dimitrov, *Cryst. Growth Design*, 2011, **11**, 196-202.
- 19 H. G. Liao, D. Zhrebetsky, H. Xin, C. Czarnik, P. Ercius, H. Elmlund, M. Pan, L. W. Wang and H. Zheng, *Science*, 2014, **345**, 916-919.
- 20 M. Jeong, J. M. Yuk and J. Y. Lee, *Chem. Mater.*, 2015, **27**, 3200-3202.
- 21 A. Kumar and V. Molinero, *J. Phys. Chem. Lett.*, 2018, **9**, 5692-5697.
- 22 N. Krautwurst, L. Nicoleau, M. Dietzsch, I. Lieberwirth, C. Labbez, A. Fernandez-Martinez, A. E. Van Driessche, B. Barton, S. Leukel and W. Tremel, *Chem. Mater.*, 2018, **30**, 2895-2904.
- 23 G. M. Hernandez and F. Renard, *Cryst. Growth Design*, 2016, **16**, 7218-7230.
- 24 J. Ihli, Y. W. Wang, B. Cantaert, Y. Y. Kim, D. C. Green, P. H. Bomans, N. A. J. M. Sommerdijk and F. C. Meldrum, *Chem. Mater.*, 2015, **27**, 3999-4007.
- 25 M. H. Nielsen, S. Aloni and J. J. De Yoreo, *Science*, 2014, **345**, 1158-1162.
- 26 T. H. Zhang and X. Y. Liu, *Angew. Chem. Int. Edit.*, 2009, **48**, 1308-1312.
- 27 T. H. Zhang and X. Y. Liu, *J. Am. Chem. Soc.*, 2007, **129**, 13520-13526.
- 28 S. Mintova, N. H. Olson, V. Valtchev and T. Bein, *Science*, 1999, **283**, 958-960.

- 29 J. Scheck, L. M. Fuhrer, B. Wu, M. Drechsler and D. Gebauer, *Chem. Eur. J.*, 2019, **25**, 13002-13007.
- 30 Y. Kimura, H. Niinomi, K. Tsukamoto and J. M. Garcia-Ruiz, *J. Am. Chem. Soc.*, 2014, **136**, 1762-1765.
- 31 W. J. Habraken, J. Tao, L. J. Brylka, H. Friedrich, L. Bertinetti, A. S. Schenk, A. Verch, V. Dmitrovic, P. H. Bomans, P. M. Frederik, J. Laven, P. van der Schoot, B. Aichmayer, G. de With, J. J. DeYoreo and N. A. J. M. Sommerdijk, *Nat. Commun.*, 2013, **4**, 1507.
- 32 A. R. Finney and P. M. Rodger, *Faraday Discuss.*, 2012, **159**, 47-60.
- 33 A. Dey, P. H. Bomans, F. A. Muller, J. Will, P. M. Frederik, G. de With and N. A. J. M. Sommerdijk, *Nat. Mater.*, 2010, **9**, 1010-1014.
- 34 D. Gebauer, A. Völkel and H. Cölfen, *Science*, 2008, **322**, 1819-1822.
- 35 S. L. Wolf, L. Caballero, F. Melo and H. Cölfen, *Langmuir*, 2017, **33**, 158-163.
- 36 S. E. Wolf, J. Leiterer, V. Pipich, R. Barrea, F. Emmerling and W. Tremel, *J. Am. Chem. Soc.*, 2011, **133**, 12642-12649.
- 37 M. Olszta, E. Douglas and L. B. Gower, *Calcif. Tissue Int.*, 2003, **72**, 583-591.
- 38 T. Kato, *Adv. Mater.*, 2000, **12**, 1543-1546.
- 39 L. B. Gower and D. J. Odom, *J. Cryst. Growth*, 2000, **210**, 719-734.
- 40 E. Wiedenbeck, M. Kovermann, D. Gebauer and H. Cölfen, *Angew. Chem. Int. Edit.*, 2019, **58**, 19103-19109.
- 41 M. S. Safari, Z. Wang, K. Tailor, A. B. Kolomeisky, J. C. Conrad and P. G. Vekilov, *iScience*, 2019, **12**, 342-355.
- 42 R. Schubert, A. Meyer, D. Baitan, K. Dierks, M. Perbandt and C. Betzel, *Cryst. Growth Design*, 2017, **17**, 954-958.
- 43 P. G. Vekilov, *Cryst. Growth Design*, 2004, **4**, 671-685.
- 44 A. Ianiro, H. Wu, M. M. J. van Rijt, M. P. Vena, A. D. A. Keizer, A. C. C. Esteves, R. Tuinier, H. Friedrich, N. A. J. M. Sommerdijk and J. P. Patterson, *Nat. Chem.*, 2019, **11**, 320-328.
- 45 H. Ding, H. Pan, X. Xu, R. Tang, *Cryst. Growth Design*, 2014, **14**, 763-769.
- 46 S. Chung, S. H. Shin, C. R. Bertozzi and J. J. De Yoreo, *Proc. Natl. Acad. Sci. U S A*, 2010, **107**, 16536-16541.
- 47 J. M. Yuk, Q. Zhou, J. Chang, P. Ercius, A. P. Alivisatos and A. Zettl, *ACS Nano*, 2016, **10**, 88-92.
- 48 H. Jiang, P. G. Debenedetti and A. Z. Panagiotopoulos, *J. Chem. Phys.*, 2019, **150**, 124502.
- 49 J. T. Avaro, S. L. Wolf, K. Hauser and D. Gebauer, *Angew. Chem. Int. Edit.*, 2020, **132**, 6212-6217.
- 50 F. Sebastiani, S. L. Wolf, B. Born, T. Q. Luong, H. Cölfen, D. Gebauer and M. Havenith, *Angew. Chem. Int. Edit.*, 2017, **56**, 490-495.
- 51 T. Zhu, B. Zhang, J. Zhang, J. Lu, H. Fan, N. Rowell, J. A. Ripmeester, S. Han and K. Yu, *Chem. Mater.*, 2017, **29**, 5727-5735.
- 52 C. Rodriguez-Navarro, A. Burgos Cara, K. Elert, C. V. Putnis and E. Ruiz-Agudo, *Cryst. Growth Design*, 2016, **16**, 1850-1860.
- 53 F. M. Ross, *Liquid Cell Electron Microscopy*, Cambridge University Press, 2016.
- 54 J. Baumgartner, A. Dey, P. H. H. Bomans, C. Le Coadou, P. Fratzl, N. A. J. M. Sommerdijk and D. Faivre, *Nat. Mater.*, 2013, **12**, 310-314.
- 55 M. Kellermeier, D. Gebauer, E. Melero-García, M. Drechsler, Y. Talmon, L. Kienle, H. Cölfen, J. M. Garcia-Ruiz and W. Kunz, *Adv. Funct. Mater.*, 2012, **22**, 4301-4311.
- 56 S. G. Kwon and T. Hyeon, *Small*, 2011, **7**, 2685-2702.
- 57 M. Sleutel, J. Lutsko, A. E. Van Driessche, M. A. Duran-Olivencia and D. Maes, *Nat. Commun.*, 2014, **5**, 5598.
- 58 G. Bai, D. Gao, Z. Liu, X. Zhou and J. Wang, *Nature*, 2019, **576**, 437-441.
- 59 P. J. Smeets, K. R. Cho, R. G. Kempen, N. A. J. M. Sommerdijk and J. J. De Yoreo, *Nat. Mater.*, 2015, **14**, 394-399.
- 60 J. Park, H. Elmlund, P. Ercius, J. M. Yuk, D. T. Limmer, Q. Chen, K. Kim, S. H. Han, D. A. Weitz and A. Zettl, *Science*, 2015, **349**, 290-295.
- 61 T. Yamazaki, Y. Kimura, P. G. Vekilov, E. Furukawa, M. Shirai, H. Matsumoto, A. E. Van Driessche and K. Tsukamoto, *Proc. Natl. Acad. Sci. U S A*, 2017, **114**, 2154-2159.
- 62 S. Jiang, H. Pan, Y. Chen, X. Xu and R. Tang, *Faraday Discuss.* 2015, **179**, 451-461.
- 63 B. Jin, Y. Wang, Z. Liu, A. France-Lanord, J. C. Grossman, C. Jin and R. Tang, *Adv. Mater.*, 2019, **31**, 1808225.
- 64 N. D. Loh, S. Sen, M. Bosman, S. F. Tan, J. Zhong, C. A. Nijhuis, P. Kral, P. Matsudaira and U. Mirsaidov, *Nat. Chem.*, 2017, **9**, 77-82.
- 65 L. A. Wills, X. Qu, I. Y. Chang, T. J. L. Mustard, D. A. Keszler, K. A. Persson and P. H. Cheong, *Nat. Commun.*, 2017, **8**, 15852.
- 66 C. M. Volkle, D. Gebauer and H. Cölfen, *Faraday Discuss.*, 2015, **179**, 59-77.
- 67 M. Kellermeier, P. Raiteri, J. K. Berg, A. Kempter, J. D. Gale and D. Gebauer, *Chem. Phys. Chem.*, 2016, **17**, 3535-3541.
- 68 J. Zhang, Y. Sun and J. Yu, *J. Cryst. Growth*, 2017, **478**, 77-84.
- 69 A. Burgos-Cara, C. V. Putnis, C. Rodriguez-Navarro and E. Ruiz-Agudo, *Minerals*, 2017, **7**, 126.
- 70 M. Salvalaglio, C. Perego, F. Giberti, M. Mazzotti and M. Parrinello, *Proc. Natl. Acad. Sci. U S A*, 2015, **112**, E6-14.
- 71 E. Ruiz-Agudo, A. Burgos-Cara, C. Ruiz-Agudo, A. Ibanez-Velasco, H. Colfen and C. Rodriguez-Navarro, *Nat. Commun.*, 2017, **8**, 768.
- 72 N. A. Garcia, R. I. Malini, C. L. Freeman, R. Demichelis, P. Raiteri, N. A. J. M. Sommerdijk, J. H. Harding and J. D. Gale, *Cryst. Growth Design*, 2019, **19**, 6422-6430.
- 73 R. Innocenti Malini, C. L. Freeman and J. H. Harding, *Cryst. Eng. Commun.*, 2019, **21**, 6354-6364.
- 74 X. Yang, M. Wang, Y. Yang, B. Cui, Z. Xu and X. Yang, *Phys. Chem. Chem. Phys.*, 2019, **21**, 14530-14540.
- 75 B. Das, *J. Phys. Chem. A*, 2018, **122**, 652-661.
- 76 J. Scheck, B. Wu, M. Drechsler, R. Rosenberg, A. E. Van Driessche, T. M. Stawski and D. Gebauer, *J. Phys. Chem. Lett.*, 2016, **7**, 3123-3130.
- 77 H. J. Li, D. Yan, H. Q. Cai, H. B. Yi, X. B. Min and F. F. Xia, *Phys. Chem. Chem. Phys.*, 2017, **19**, 11390-11403.
- 78 D. Gebauer and H. Cölfen, *Nano Today*, 2011, **6**, 564-584.
- 79 R. Demichelis, P. Raiteri, J. D. Gale, D. Quigley and D. Gebauer, *Nat. Commun.*, 2011, **2**, 1-8.
- 80 G. Mancardi, U. Terranova and N. H. de Leeuw, *Cryst. Growth Design*, 2016, **16**, 3353-3358.
- 81 R. Demichelis, N. A. Garcia, P. Raiteri, R. Innocenti Malini, C. L. Freeman, J. H. Harding and J. D. Gale, *J. Phys. Chem. B*, 2018, **122**, 1471-1483.

- 82 S. Sun, D. Gebauer and H. Cölfen, *Angew. Chem. Int. Edit.*, 2017, **56**, 4042-4046.
- 83 M. P. Andersson, S. Dobberschütz, K. K. Sand, D. J. Tobler, J. J. De Yoreo and S. L. Stipp, *Angew. Chem. Int. Edit.*, 2016, **128**, 11252-11256.
- 84 K. Henzler, E. O. Fetisov, M. Galib, M. D. Baer, B. A. Legg, C. Borca, J. M. Xto, S. Pin, J. L. Fulton and G. K. Schenter, *Sci. Adv.*, 2018, **4**, eaao6283.
- 85 Z. J. Jiang and D. F. Kelley, *ACS Nano*, 2010, **4**, 1561-1572.
- 86 M. Liu, K. Wang, L. Wang, S. Han, H. Fan, N. Rowell, J. A. Ripmeester, R. Renoud, F. Bian and J. Zeng, *Nat. Commun.*, 2017, **8**, 1-12.
- 87 D. C. Gary, M. W. Terban, S. J. L. Billinge and B. M. Cossairt, *Chem. Mater.*, 2015, **27**, 1432-1441.
- 88 C. Luan, J. Tang, N. Rowell, M. Zhang, W. Huang, H. Fan and K. Yu, *J. Phys. Chem. Lett.*, 2019, **10**, 4345-4353.
- 89 J. Zhu, L. Huang, M. Cui, L. Ma, and F. Cao, *Eur. J. Inorg. Chem.*, 2015, **10**, 1819-1826.
- 90 Y. Li, J. Zhu, M. Cui, J. Wang and J. Zha, *J. Cryst. Growth*, 2019, **507**, 362-369.
- 91 L. Dai, E. P. Douglas and L. B. Gower, *J. Non-crystalline Solids*, 2008, **354**, 1845-1854.
- 92 S. Kashyap, T. J. Woehl, X. Liu, S. K. Mallapragada and T. Prozorov, *ACS Nano*, 2014, **8**, 9097-9106.
- 93 M. Sleutel and A. E. Van Driessche, *Proc. Natl. Acad. Sci. U S A*, 2014, **111**, E546-553.
- 94 S. Wohlrab, H. Cölfen and M. Antonietti, *Angew. Chem. Int. Edit.*, 2005, **44**, 4087-4092.
- 95 Y. Y. Kim, E. P. Douglas and L. B. Gower, *Langmuir*, 2007, **23**, 4862-4870.
- 96 B. Cantaert, Y. Y. Kim, H. Ludwig, F. Nudelman, N. A. Sommerdijk and F. C. Meldrum, *Adv. Funct. Mater.*, 2012, **22**, 907-915.
- 97 A. S. Schenk, H. Zope, Y.-Y. Kim, A. Kros, N. A. Sommerdijk and F. C. Meldrum, *Faraday Discuss.*, 2012, **159**, 327-344.
- 98 S. Yao, X. Lin, Y. Xu, Y. Chen, P. Qiu, C. Shao, B. Jin, Z. Mu, N. A. J. M. Sommerdijk and R. Tang, *Adv. Sci.*, 2019, **6**.
- 99 M. A. Bewernitz, D. Gebauer, J. Long, H. Cölfen and L. B. Gower, *Faraday Discuss.*, 2012, **159**.
- 100 J. K. Berg, T. Jordan, Y. Binder, H. G. Börner and D. Gebauer, *J. Am. Chem. Soc.*, 2013, **135**, 12512-12515.
- 101 Y. Xu, K. C. Tijssen, P. H. Bomans, A. Akiva, H. Friedrich, A. P. Kentgens and N. A. J. M. Sommerdijk, *Nat. Commun.*, 2018, **9**, 1-12.
- 102 C. Yuan, A. Levin, W. Chen, R. Xing, Q. Zou, T. W. Herling, P. K. Challa, T. P. J. Knowles and X. Yan, *Angew. Chem. Int. Edit.*, 2019, **58**, 18116-18123.
- 103 P. R. ten Wolde and D. J. S. Frenkel, *Science*, 1997, **277**, 1975-1978.
- 104 P. J. Smeets, A. R. Finney, W. J. Habraken, F. Nudelman, H. Friedrich, J. Laven, J. J. De Yoreo, P. M. Rodger and N. A. J. P. Sommerdijk, *Proc. Natl. Acad. Sci. U S A*, 2017, **114**, E7882-E7890.
- 105 A. F. Wallace, L. O. Hedges, A. Fernandez-Martinez, P. Raiteri, J. D. Gale, G. A. Waychunas, S. Whitlam, J. F. Banfield and J. J. De Yoreo, *Science*, 2013, **341**, 885-889.
- 106 N. D. Loh, S. Sen, M. Bosman, S. F. Tan, J. Zhong, C. A. Nijhuis, P. Král, P. Matsudaira and U. Mirsaidov, *Nat. Chem.*, 2016, **9**, 77.
- 107 J. F. Lutsko, *Sci. Adv.*, 2019, **5**, eaav7399.
- 108 M. Farhadi Khouzani, D. M. Chevrier, P. Güttlein, K. Hauser, P. Zhang, N. Hedin and D. Gebauer, *CrystEngComm*, 2015, **17**, 4842-4849.
- 109 T. Wakihara, S. Kohara, G. Sankar, S. Saito, M. Sanchez-Sanchez, A. R. Overweg, W. Fan, M. Ogura and T. J. P. C. C. P. Okubo, 2006, **8**, 224-227.
- 110 A. F. Ogata, A. M. Rakowski, B. P. Carpenter, D. A. Fishman, J. G. Merham, P. J. Hurst and J. P. Patterson, *J Am Chem Soc*, 2020, DOI: 10.1021/jacs.9b11371.
- 111 H. Pan, X. Y. Liu, R. Tang and H. Y. J. C. C. Xu, 2010, **46**, 7415-7417.
- 112 C. Li and L. Qi, *Angew. Chem. Int. Edit.*, 2008, **47**, 2388-2393.
- 113 C. E. Hughes, P. A. Williams, B. M. Kariuki and K. D. Harris, *Chem. Phys. Chem.*, 2018, **19**, 3341-3345.
- 114 J. D. Rimer, *Proc. Natl. Acad. Sci. U S A*, 2020, **117**, 3360-3362.
- 115 C. J. Stephens, S. F. Ladden, F. C. Meldrum and H. K. Christenson, *Adv. Funct. Mater.*, 2010, **20**, 2108-2115.
- 116 C. J. Stephens, Y. Y. Kim, S. D. Evans, F. C. Meldrum and H. K. Christenson, *J. Am. Chem. Soc.*, 2011, **133**, 5210-5213.
- 117 E. Seknazi, S. Kozachkevich, I. Polishchuk, N. Bianco Stein, J. Villanova, J. P. Suuronen, C. Dejoie, P. Zaslansky, A. Katsman and B. Pokroy, *Nat. Commun.*, 2019, **10**, 4559.
- 118 F. Zhu, T. Nishimura, T. Sakamoto, H. Tomono, H. Nada, Y. Okumura, H. Kikuchi and T. Kato, *Chem. Asian J.*, 2013, **8**, 3002-3009.
- 119 C. Li, G. Hong, H. Yu and L. Qi, *Chem. Mater.*, 2010, **22**, 3206-3211.
- 120 H. Chen, X. Zheng, Q. Li, Y. Yang, S. Xiao, C. Hu, Y. Bai, T. Zhang, K. S. Wong and S. Yang, *J. Mater. Chem. A*, 2016, **4**, 12897-12912.
- 121 H. Du, M. Steinacher, C. Borca, T. Huthwelker, A. Murello, F. Stellacci and E. Amstad, *J. Am. Chem. Soc.*, 2018, **140**, 14289-14299.
- 122 H. Du and E. Amstad, *Angew. Chem. Int. Edit.*, 2019, **59**, 1798-1816.
- 123 Y. U. Gong, C. E. Killian, I. C. Olson, N. P. Appathurai, A. L. Amasino, M. C. Martin, L. J. Holt, F. H. Wilt and P. Gilbert, *Proc. Natl. Acad. Sci. U S A*, 2012, **109**, 6088-6093.
- 124 A. Radha, T. Z. Forbes, C. E. Killian, P. Gilbert and A. Navrotsky, *Proc. Natl. Acad. Sci. U S A*, 2010, **107**, 16438-16443.
- 125 A. Van Driessche, L. Benning, J. Rodriguez-Blanco, M. Ossorio, P. Bots and J. Garcia-Ruiz, *Science*, 2012, **336**, 69-72.
- 126 T. M. Stawski, A. E. van Driessche, M. Ossorio, J. Diego Rodriguez-Blanco, R. Besselink and L. G. Benning, *Nat. Commun.*, 2016, **7**, 11177.
- 127 A. Navrotsky, *Proc. Natl. Acad. Sci. U S A*, 2004, **101**, 12096-12101.
- 128 G. Klaerner and R. Padmanabhan, *Reference Module in Materials Science and Materials Engineering*, 2016, DOI: 10.1016/b978-0-12-803581-8.03768-1.
- 129 T. C. Michaels, H. W. Lazell, P. Arosio and T. P. Knowles, *J. Chem. Phys.*, 2015, **143**, 054901.
- 130 W. S. Wei, Y. Xia, S. Ettinger, S. Yang and A. G. Yodh, *Nature*, 2019, **576**, 433-436.
- 131 K. Kajihara, *J. Asian Ceram. Soc.*, 2018, **1**, 121-133.
- 132 A. Shimojima and K. Kuroda, *Angew. Chem. Int. Edit.*, 2003, **42**, 4057-4060.

- 133 C. H. Lin, J. H. Chang, Y. Q. Yeh, S. H. Wu, Y. H. Liu and C. Y. Mou, *Nanoscale*, 2015, **7**, 9614-9626.
- 134 Q. Yue, J. Li, W. Luo, Y. Zhang, A. A. Elzatahry, X. Wang, C. Wang, W. Li, X. Cheng, A. Alghamdi, A. M. Abdullah, Y. Deng and D. Zhao, *J. Am. Chem. Soc.*, 2015, **137**, 13282-13289.
- 135 D. Li, R. Yi, J. Tian, J. Li, B. Yu and J. Qi, *Chem. Commun.*, 2017, **53**, 8902-8905.
- 136 W. E. Muller, H. C. Schroder, Z. Burghard, D. Pisignano and X. Wang, *Chemistry*, 2013, **19**, 5790-5804.
- 137 A. K. Meka, P. L. Abbaraju, H. Song, C. Xu, J. Zhang, H. Zhang, M. Yu and C. Yu, *Small*, 2016, **12**, 5169-5177.
- 138 Z. Liu, C. Shao, B. Jin, Z. Zhang, Y. Zhao, X. Xu and R. Tang, *Nature*, 2019, **574**, 394-398.
- 139 C. Shao, B. Jin, Z. Mu, H. Lu, Y. Zhao, Z. Wu, L. Yan, Z. Zhang, Y. Zhou and H. J. S. Pan, *Sci. Adv.*, 2019, **5**, eaaw9569.
- 140 P. Raiteri and J. D. Gale, *Proc. Natl. Acad. Sci. U S A*, 2010, **132**, 17623-17634.
- 141 B. Jin, Y. Wang, Z. Liu, A. France-Lanord, J. C. Grossman, C. Jin and R. Tang, *Adv. Mater.*, 2019, **31**, e1808225.
- 142 A. Dey and N. A. J. M. Sommerdijk, *Chem. Soc. Rev.*, 2010, **39**, 397-409.
- 143 A. S. Myerson and B. L. Trout, *Science*, 2013, **341**, 855-856.

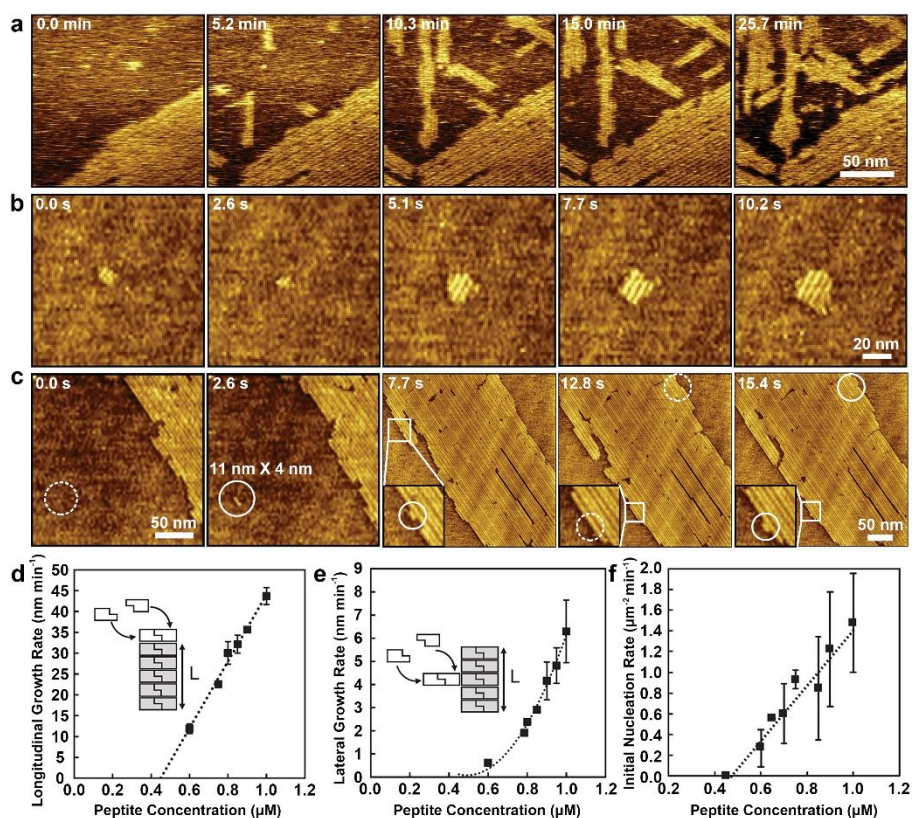


Figure 1. In situ AFM showing the nucleation and growth dynamics of MoSBP1 on MoS₂ (0001). (a) The direct growth process of peptides by attaching to the surface and growing into ordered structures. (b) The formation and development of a small island; (c) Nucleation of a single row (0.0 s and 2.6 s) and creation of new rows adjacent to existing ones (7.7 s to 15.4 s). Circles highlight regions where new rows appear (dashed, before; solid, after). (d to f) Longitudinal (d) and lateral (e) island growth rates and initial nucleation rate (f) versus peptide concentration. Reprinted with permission from ref. 10. Copyright 2018, American Association for the Advancement of Science.

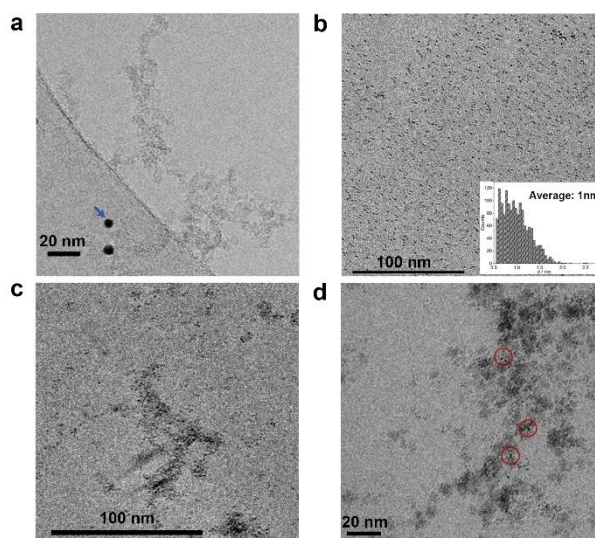


Figure 2. Cryo-TEM revealing the formation and aggregation of clusters. (a) High-resolution cryo-TEM image of assemblies of calcium phosphate clusters in SBF kept at 37 °C for 24 h. Reprinted with permission from ref. 33. (b-c) Polydisperse (1–2 nm) iron (III) (oxyhydr)oxide species, which qualify as clusters at prenucleation stage. The inset shows the clusters size distribution. (c) The aggregation of clusters in the transition stage. Reprinted with permission from ref. 76. Copyright 2016, American Chemical Society. (d) The hematite particles consisting of small species (red circles) that formed from PNCs on phase separation. Reprinted with permission from ref. 29. Copyright 2019, Wiley-VCH.



Figure 3. Cryo-TEM characterization of PILP phase. (a) Approximately 30 nm-sized nanoparticles. The inset is a zoom-in image showing the ~2 nm-sized subunits. Reprinted with permission from ref. 101. Copyright 2018, Springer Nature. (b) The viscous but still free flowing calcium phosphate-PILP; (b) Reconstruction of a cryo-TEM image shows homogeneously distributed and separated nanoclusters within calcium phosphate-PILP. Inset 1 is a zoomed-in cryo-TEM image; SAED pattern in inset 2 shows amorphous clusters. Reprinted with permission from ref. 98. Copyright 2019, Wiley-VCH.

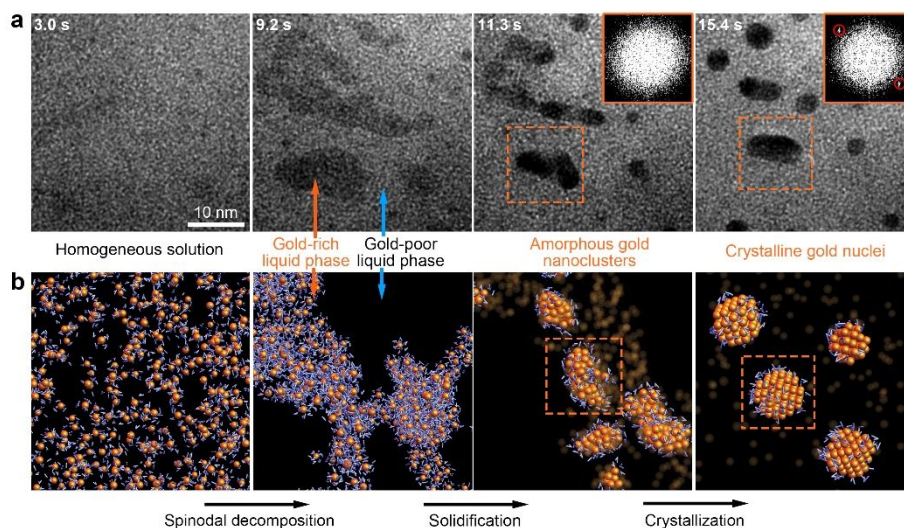


Figure 4. The multiple nucleation process of Au nanocrystals in aqueous solution revealed by liquid-cell TEM. (a) A series of TEM images that shows the intermediate steps in nucleating gold nanocrystals from a supersaturated aqueous Au⁰ solution. Insets show Fourier transforms of cropped square regions (orange) with the Au (111) fcc reciprocal lattice spacing circled in red; (b) Schematic of the proposed steps in nucleation (gold as orange spheres, with surrounding water as blue bent lines). Reprinted with permission from ref. 106.

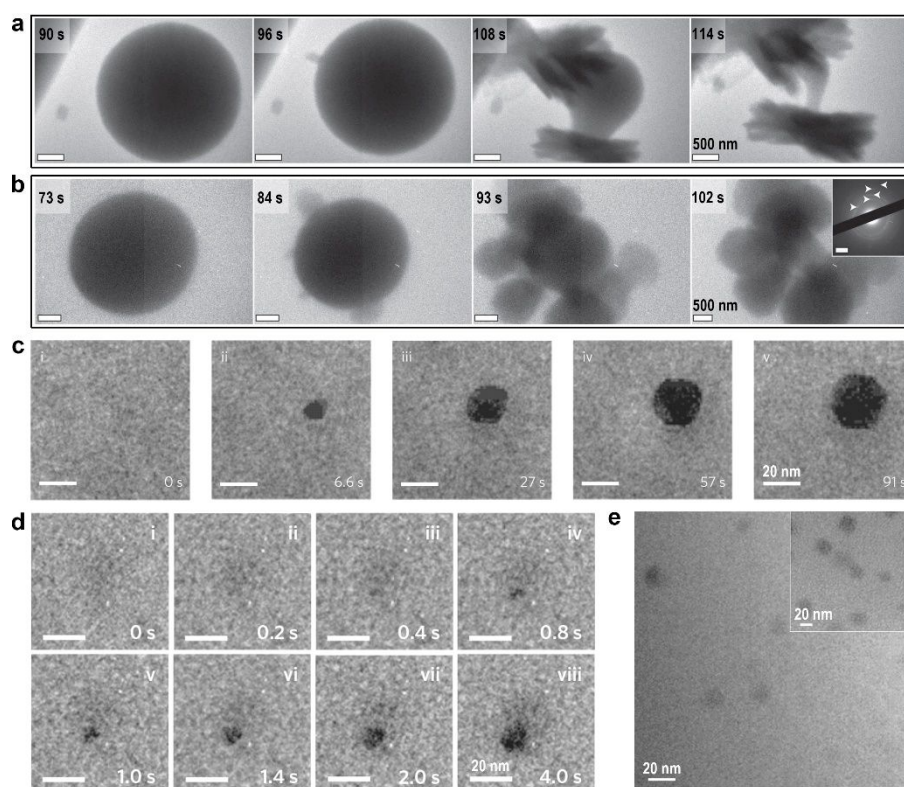


Figure 5. In situ TEM revealing the nucleation process of CaCO₃ in solution. (a, b) The direct transformation of ACC to aragonite (a) and vaterite (b); (c) The direct nucleation and growth of vaterite from solution. Reprinted with permission from ref. 25. Copyright 2014, American Association for the Advancement of Science. (d) Initial nucleation and growth of a CaCO₃ particle inside or on a primary Ca-PSS globule; (e) Large PSS-Ca globules in liquid. Reprinted with permission from ref. 59.

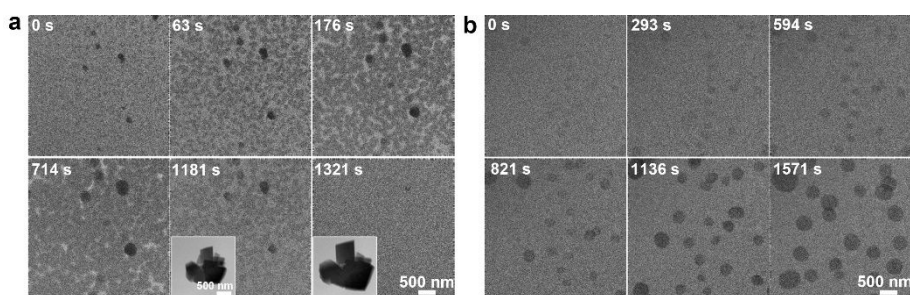


Figure 6. Liquid-cell TEM observing the nucleation and growth process of CaCO_3 . (a) Growth of ACC particles with 2.5 mM Mg^{2+} and their subsequent dissolution. All particles in the main panels are ACC. (Inset) In situ images of growing calcite particles via dissolution and recrystallization; (b) Growth and direct solid-solid transformation of ACC particles to calcite in the presence of 5.0 mM Mg^{2+} . Reprinted with permission from ref. 13. Copyright 2020, National Academy of Science.

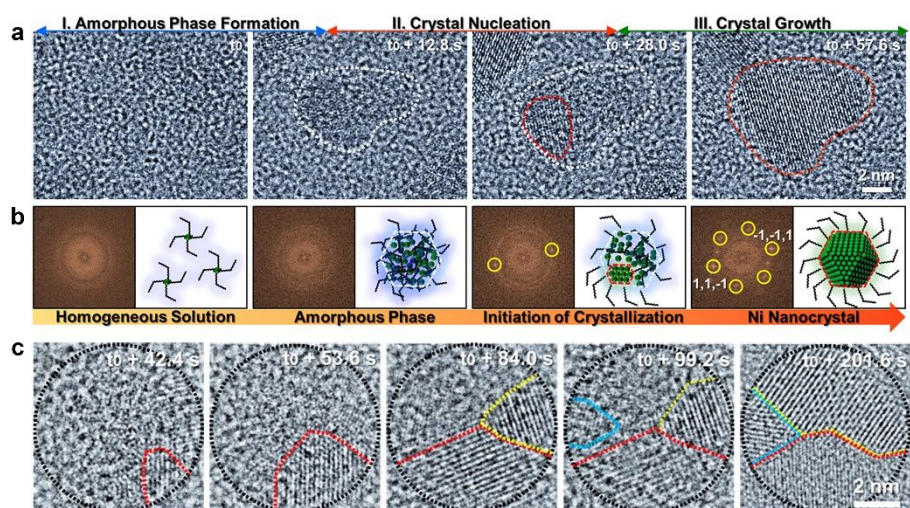


Figure 7. In situ liquid-cell TEM showing the amorphous phase mediated formation process of Ni Nanocrystals. (a) The reaction stages of amorphous-phase-mediated crystallization. The white and red dashed lines represent the amorphous and crystalline phases, respectively; (b) The corresponding FFT images and schematic illustrations; (c) A time series of TEM images showing multiple nucleation sites within an amorphous particle. The coloured lines highlight three crystalline domains. Reprinted with permission from ref. 12. Copyright 2019, American Chemical Society.

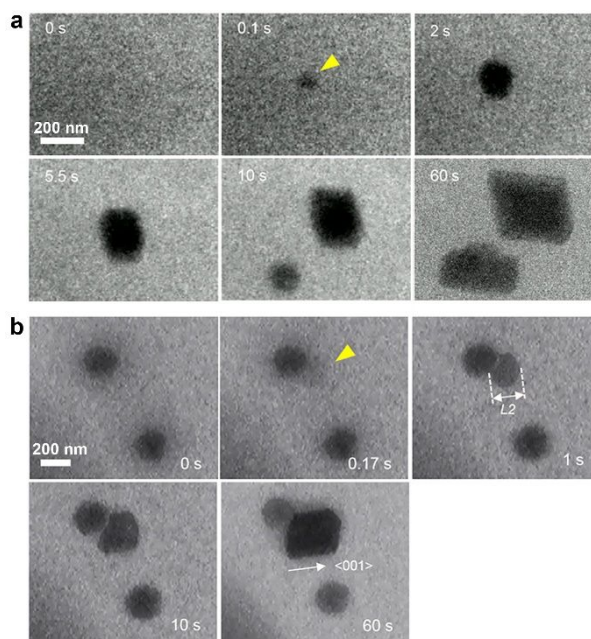


Figure 8. In situ liquid-cell TEM showing the nucleation of lysozyme crystals. (a) A spherical amorphous particle observed at 0.1 s (yellow arrowhead) transforms into an orthorhombic crystal; (b) A spherical particle, indicated with a yellow arrowhead, forms at 0.17 s near an amorphous solid particle and transforms into an orthorhombic crystal. Reprinted with permission from ref. 61. Copyright 2017, National Academy of Science.

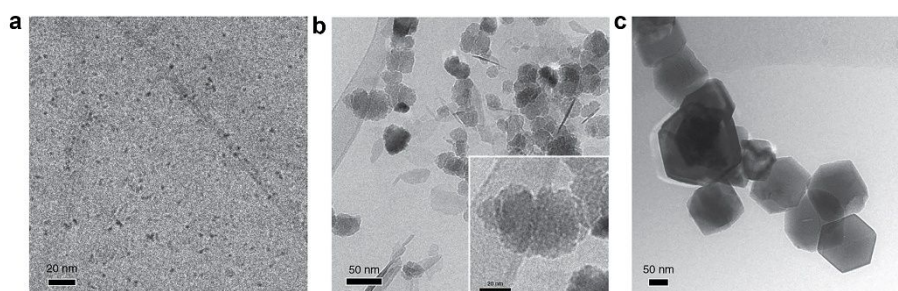


Figure 9. Cryo-TEM images of different stages of magnetite formation. (a) The formation of primary particles; (b) The aggregated of primary particles. Inset is magnified cryo-TEM image of aggregates; (c) The final magnetite crystals. Reprinted with permission from ref. 6. Copyright 2019, Springer Nature.

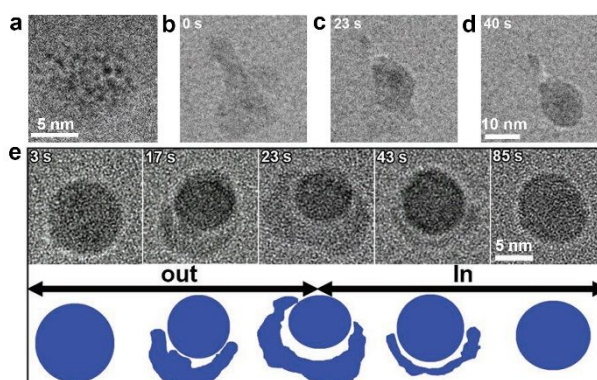


Figure 10. Liquid-cell TEM revealing the nucleation and relaxation of Pd nanocrystals. (a) The early stage structure before the cluster-cloud formation, showing the existence of nanoclusters; (b) The formation of cluster-cloud; (c, d) The condensation of cluster-cloud into a nanoparticles; (e) The typical cluster-cloud relaxation mechanism of “out” and “in” processes. Reprinted with permission from ref. 63. Copyright 2019, Wiley-VCH.

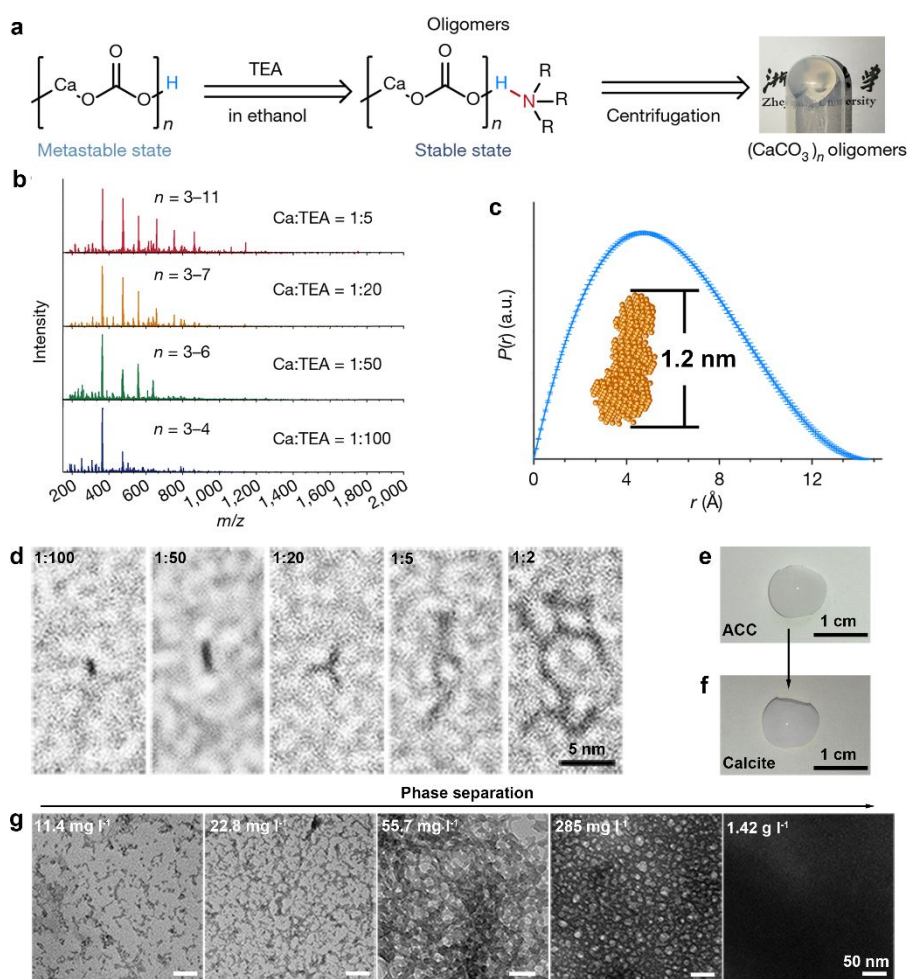


Figure 11. The synthesized CaCO_3 oligomers. (a) Scheme of the capping strategy and reaction conditions for producing $(\text{CaCO}_3)_n$ oligomers (Left) and a photograph of gel-like oligomers (Right); (b) Mass spectra of $(\text{CaCO}_3)_n$ oligomers with different Ca/TEA molar ratios; (c) Pair-distance distribution function $P(r)$ of the $(\text{CaCO}_3)_n$ oligomers. The inset shows the shape simulation of the oligomer; (d) High-resolution TEM images of $(\text{CaCO}_3)_n$ oligomers grown at different Ca:TEA ratios from 1:100 to 1:2; (e, f) Photographs of monolithic ACC prepared from $(\text{CaCO}_3)_n$ oligomers (e) and monolithic calcite prepared from monolithic ACC (f); (g) TEM images showing the transformation of $(\text{CaCO}_3)_n$ oligomers to larger structures during condensation. Reprinted with permission from ref. 138. Copyright 2020, Springer Nature.

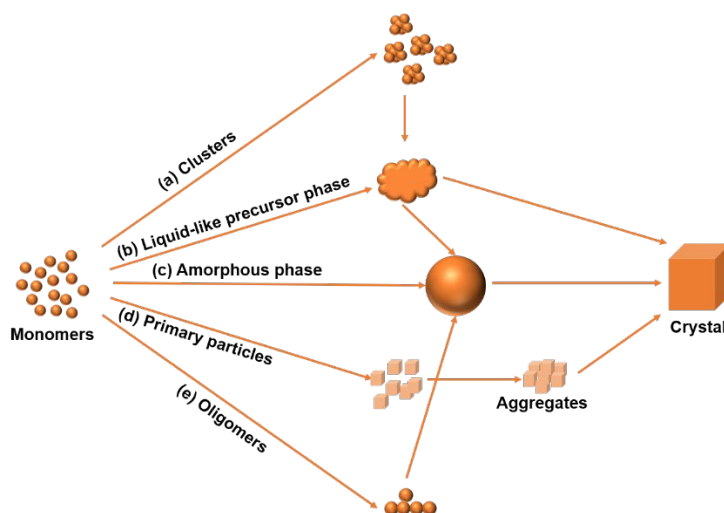


Figure 12. Schematic representation of the possible nucleation pathways. (a) cluster-mediated nucleation pathway. (b) Liquid-like phase as precursor for nucleation. (c) Amorphous phase as intermediated phase in nucleation. (d) Primary particle-mediated nucleation process; (e) Oligomers mediated inorganic polymerization and crosslinking for crystal formation.



Biao Jin completed his undergraduate programme at Hainan University and received his B.E. in 2014. He received his Ph.D. in Department of Chemistry from Zhejiang University in 2019. During his Ph.D., he studied liquid-cell transmission electron microscopy in the Centre of Electron Microscopy of Zhejiang University. As a post-doctoral research fellow at Pacific Northwest National Laboratory as, his current research interests focus on nucleation and growth mechanism of nanomaterials and in situ transmission electron microscopy techniques.



Zhaoming Liu received his B.Sc. and Ph.D. degrees in the Department of Chemistry from Zhejiang University in 2013 and 2017. He is currently a research fellow at Department of Chemistry of Zhejiang University. His research focuses on crystal growth and materials science.



0, 1-3

This journal is © The Royal Society of Chemistry 20xx

Ruikang Tang studied chemistry at Nanjing University and completed his Ph.D. in 1998. Subsequently, he worked at the State University of New York at Buffalo as a postdoctoral research fellow and research assistant professor. He is currently a professor in the department of Chemistry at Zhejiang University and the State Key Laboratory of Silicon Materials. In 2006, he established the Center for Biomaterials and Biopathways and became a Changjiang Scholar Chair Professor of the Ministry of Education of China. His research focuses on biomineralization, biomaterials and biomimetic pathways.

TOC figure

This work provides a clearer picture for non-classical nucleation via revealing the presence of various intermediates using advanced characterization techniques.

